

Stimulated emission from the biexciton in a single quantum dot

I. A. Akimov, J. T. Andrews, and F. Henneberger

Humboldt Universität zu Berlin, Institut für Physik, Newtonstr.15, 12489 Berlin, Germany

(Dated: January 1, 2022)

Using two optical pulses of different frequencies, we demonstrate entanglement and disentanglement of the electronic states in Stranski-Krastanov quantum dots. Resonant two-photon excitation of the biexciton creates an entangled Bell-like state. The second pulse, being resonant to the exciton-biexciton transition, stimulates the emission from the biexciton and fully disentangles the two-bit system. By setting the polarization of the stimulation pulse, we control the recombination path of the biexciton and, by this, the state of the photons emitted in the decay cascade.

PACS numbers: 42.50.Md, 78.67.Hc, 78.55.Et

Entangled states and their manipulation play an important role in quantum information processing [1]. A state of a pair of quantum systems is said to be entangled if it cannot be factored into the states of the individual subsystems. When aiming at practical devices, implementations in solid state are of particular interest. Here, a critical issue is decoherence that destroys the non-classical quantum correlations.

Semiconductor quantum dots (QDs) with electronic excitations localized on a nanometer length scale have recently attracted much attention as building blocks for quantum logic [2, 3]. The two-exciton subspace of a QD is spanned by the ground-state $|g\rangle$ (no exciton), the single-exciton states, and the biexciton state $|b\rangle$. The optically active exciton is split by anisotropy in two linearly cross-polarized components $|x\rangle$ and $|y\rangle$ [4]. Thus, identifying $|00\rangle = |g\rangle$, $|10\rangle = |x\rangle$, $|01\rangle = |y\rangle$, and $|11\rangle = |b\rangle$, a two-bit system is built. The optical couplings between those states form the V- Λ transition scheme of Fig. 1a, where the exciton-biexciton resonances are low-energy shifted from that of the single excitons by the exciton-exciton interaction energy ΔE_{XX} in the biexciton.

Coherent optical coupling of the ground-state and the biexciton creates an entangled state of the type $a_{00}|00\rangle + a_{11}|11\rangle$ [5, 6]. A Bell state of maximum entanglement is achieved if $|a_{ii}| = \frac{1}{\sqrt{2}}$. Excitation of the biexciton $|g\rangle \rightarrow |b\rangle$ requires two photons. In Ref.[7], two non-degenerate beams, each being resonant to one of the single-photon transitions, e.g. $|g\rangle \rightarrow |x\rangle$ and $|x\rangle \rightarrow |b\rangle$, have been utilized. The present study is based on resonant two-photon (TP) excitation [8]. That approach, where the degenerate photons have half the energy of the biexciton, has the advantage that the spontaneous emission from the cascaded biexciton-exciton decay is clearly separated from the excitation stray light and can thus be used as a monitor of the quantum dynamics. The ability to track the QD emission is essential, as it enables to generate non-classical light states, like anti-bunched single-photon emission [9] or entangled photon pairs [10].

In what follows we demonstrate that an entangled state in the two-exciton subspace of a QD can be indeed created by resonant TP excitation. The entanglement of formation reaches values of about 0.5. In a next step, we accomplish the conversion of the biexciton into an exciton

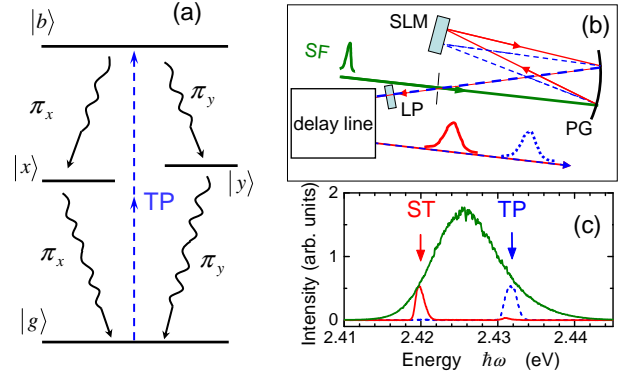


FIG. 1: (a) Schematics of the exciton-biexciton system in a QD. For explanations see text. (b) Layout of the pulse shaper. SF: sub-ps source pulse, SLM: spatial light modulator, PG: parabolic grating, LP: linear polarizer. (c) Spectra of the ingoing SF pulse and the resulting ST and TP pulse.

by stimulated emission applying a second pulse that is tuned to the exciton-biexciton resonance. In this way, the recombination path is strictly defined by the polarization of the stimulation pulse, in contrast to the spontaneous emission cascade. In a quantum information sense, the stimulated emission corresponds to a disentanglement of the Bell-like state $a_{00}|00\rangle + a_{11}|11\rangle \rightarrow (a_{00}|0\rangle + a_{11}|1\rangle)|0\rangle$. Disentanglement is a key step in conditional quantum dynamics and logical gates [11]. We find efficiencies of close to 1 in our measurements.

The Stranski-Krastanov CdSe/ZnSe QD structures are grown by molecular beam epitaxy [12]. II-VI QDs are favored in the present context by the large $\Delta E_{XX} \approx 20$ meV [13], allowing the use of ultra-short pulses without losing spectral selectivity of the excitation process. In order to study individual QDs, mesa structures with an area down to 100×100 nm² are fabricated. The sum frequency of a Kerr-lens mode-locked Ti:sapphire laser and a synchronously pumped optical parametric oscillator are used to generate spectrally broad sub-ps pulses with 76 MHz repetition rate in the spectral region of interest. Two spectrally narrow pulses for selective TP excitation and stimulation (ST) of the biexciton are ob-

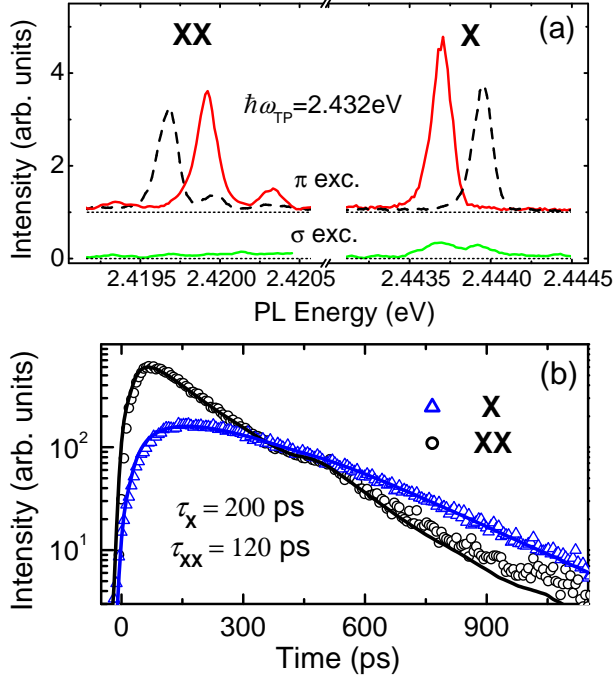


FIG. 2: (a) Exciton (X) and biexciton (XX) emission lines from a single QD under circularly (σ) and linearly (π) polarized TP excitation. The polarization detection is along (solid) and perpendicular (dashed) to the intrinsic polarization $\vec{\pi}_x$. (b) Decay transients of biexciton and exciton emission under TP excitation. Solid lines are a double-exponential data fits accounting for the apparatus function.

tained by a pulse shaper based on a programmable reflective spatial light modulator (Fig. 1b). The outgoing pulses are spatially separated and passed through a delay line. The pulse durations are about 1.0 ps (TP) and 1.5 ps (ST) and the spectral full widths at half maximum are 1.7 meV and 1.2 meV, respectively (Fig. 1c). The secondary emission of the QD is collected in a confocal arrangement and dispersed in a triple spectrometer (0.23 nm/mm) equipped with a nitrogen cooled charged coupled device. For time-resolved measurements, only the two first stages are utilized in subtractive mode (0.7 nm/mm). A multi-channel-plate photomultiplier in conjunction with time-correlated single-photon counting unit provides an overall time resolution of 60 ps. Polarization control is achieved by quarter-wave or half-wave plates, placed in the path of both the linearly polarized excitation light as well as the emission signal. The polarization of the emission is analyzed by a Glan-Thomson prism introduced in front of the spectrometer. All measurements are carried out at temperatures of about 10 K.

The cascaded spontaneous emission of a QD subsequent to TP excitation is depicted in Fig. 2. For linearly polarized excitation, distinct exciton and biexciton features, placed symmetrically to the excitation photon energy, are present. In full accord with the transition scheme of Fig. 1 a, both features consist of a fine struc-

ture doublet of linearly cross-polarized lines, however, with a reversed sequence of the polarization in the exciton and biexciton emission. The TP transition of the biexciton is forbidden for circular excitation polarization. While the emission yield decreases indeed by one order of magnitude, a weak rest emission at the exciton survives. This background originates from electron-hole pairs off-resonantly excited in the energy continuum of the heterostructure and captured by the QD. On the other hand, under linearly polarized excitation, the emission signal at the exciton lines is entirely insensitive on the polarization direction, excluding that the TP pulse addresses directly the exciton states to a measurable extent. A flip between $|x\rangle$ and $|y\rangle$ takes place on a time-scale markedly longer than the life-time and can be thus ignored [14]. The time-resolved emission shown in Fig. 2b clearly confirms the existence of an emission cascade, with the biexciton recombining first and with a respective rise time for the exciton. Double-exponential fits yield that the radiative life-time of the biexciton ($\tau_{XX} = 120$ ps) is about two times shorter than for the exciton ($\tau_X = 200$ ps). Since the biexciton has two recombination channels this means that the exciton and the exciton-biexciton transition possesses almost the same dipole moment. Using $d^2 = 3\pi\epsilon_0\hbar c^3/n_r\omega_0^3\tau$, we find $d = 27$ Debye.

Now we focus on the stimulated emission of the biexciton. In these measurements, the QD is excited by a sequence of TP and ST pulses, linearly co-polarized under an angle φ relative to the intrinsic polarization $\vec{\pi}_x$ and with tuneable time-delay τ . The result of the stimulation process is a photon as well as an exciton. While the photon can hardly be detected, the stimulated exciton is manifested by the photon that it emits subsequently. The data in Fig. 3a directly verify this scenario. While both exciton emission components have equal intensity for TP excitation only, the line polarized along the ST polarization is amplified at expense of the cross-polarized line when both pulses are present. During pulse delay, the biexciton state is increasingly emptied by spontaneous decay. Consistent with the radiative life-time, the transition is not longer capable of stimulated emission after about 250 ps. A measure to what extend a certain exciton state can be selected by the ST pulse is given by the induced linear polarization degree $\rho_L = (I_x - I_y)/(I_x + I_y)$, I_i being the spectrally integrated signal of $|i\rangle$. As seen in Fig. 3c, $\rho_L = 0$ for $\varphi = \pi/4$, while, exciting along the intrinsic polarization axis, ρ_L has the same absolute value, but is positive for $\varphi = 0$ and negative for $\varphi = \pi/2$. In an incoherent regime, the polarization degree is limited to $\rho_L = 0.5$, because the inversion between the biexciton and exciton population, addressed for a given ST polarization, can not exceed zero. In contrast, ρ_L clearly exceeds this limit and reaches values of up to 0.8 for the maximum pulse densities available by our set-up. Even the onset of Rabi oscillations for the exciton-biexciton transition is evidenced in Fig. 3b. The relatively large fine structure splitting of the exciton allows us to spectrally separate spontaneous and stimulated emission. For

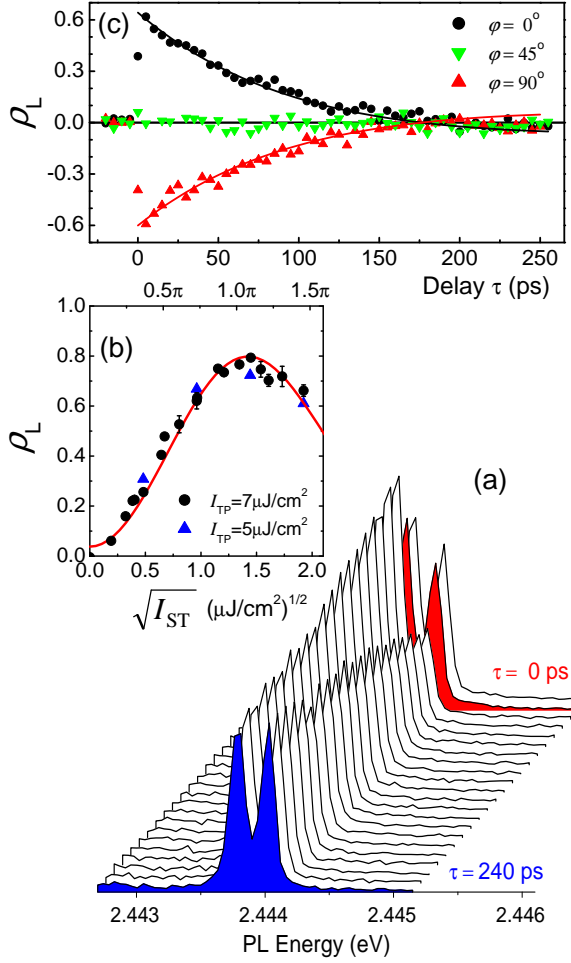


FIG. 3: (a) Evolution of exciton emission spectrum as a function of the delay τ between TP and ST pulse. The ST polarization is along the polarization of the low-energy line. (b) Induced linear polarization degree ρ_L versus square-root pulse-density $\sqrt{I_{ST}}$ ($\tau = 5$ ps, $\varphi = 0$). (c) ρ_L versus τ for ($I_{TP} = 7 \mu\text{J}/\text{cm}^2$, $I_{ST} = 1.3 \mu\text{J}/\text{cm}^2$), $\varphi = \angle(\vec{e}, \vec{\pi}_x)$. Since not related to the intrinsic QD dynamics, the off-resonant background is subtracted in (b) and (c). The solid lines are fits to the data based on the numerical solution of the Master equation for the two-exciton density matrix. For details see text.

QDs where the splitting is within the homogeneous width the stimulation process can be also accomplished, but shows only up in the polarization degree.

In order to draw quantitative conclusions on the quantum dynamics behind the experimental observations, the full density matrix of the two-exciton subspace has to be considered. Its time evolution is determined by the Master equation $\hbar\dot{\rho} = [H, \rho] + \hbar\Gamma[\rho]$ with the Hamiltonian given in units of \hbar and rotating-wave approximation by

$$H = \omega_g|g\rangle\langle g| + \omega_x|x\rangle\langle x| + \omega_y|y\rangle\langle y| + \omega_b|b\rangle\langle b| \\ - \frac{1}{2}\{\Omega(t)e^{-i\omega t}[\cos(\varphi)(|x\rangle\langle g| + |b\rangle\langle x|) \\ + \sin(\varphi)(|y\rangle\langle g| + |b\rangle\langle y|)] + \text{h.c.}\}$$

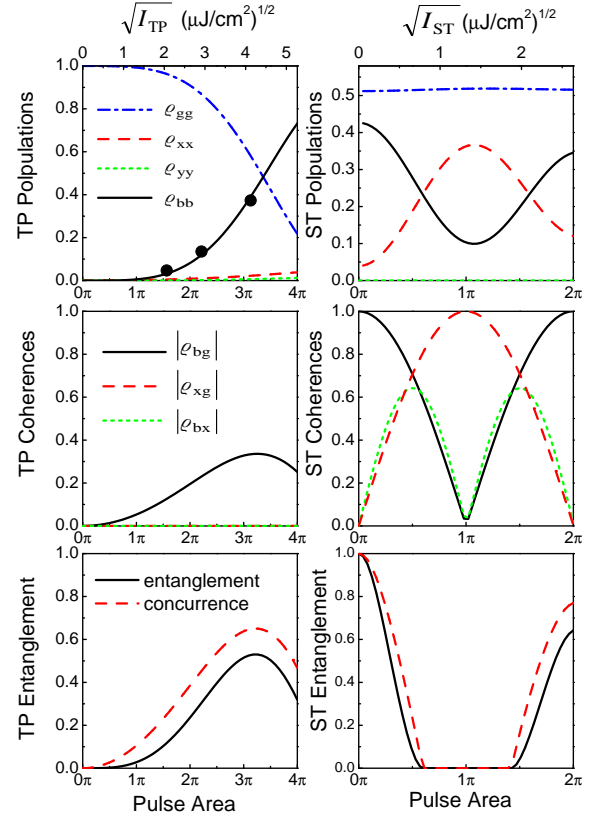


FIG. 4: Calculated populations, coherences, entanglement, and concurrence versus pulse area for the TP (left) and the ST pulse (right). The experimental points in the left top panel represent the normalized signal of the XX emission under TP excitation only. The plots in the two lower-right panels are normalized with respect to the initial values produced by the TP pulse. $\tau = 5$ ps, $\theta_{TP} = 3\pi$.

$\Omega = \frac{d}{\hbar}\mathcal{E}(t)$ is the time-dependent Rabi frequency of the field amplitude $\mathcal{E}(t)$, whereby the same d is taken for all transitions. Expressed in the two-exciton basis, the Master equation defines a complete set of differential equations for the 10 independent density matrix elements $\rho_{ij} = \rho_{ji}^*$. For the relaxation terms, we use $\langle i|\Gamma[\rho]|j\rangle = -\Gamma_{ij}\rho_{ij}$ ($i \neq j$), $\langle b|\Gamma[\rho]|b\rangle = -\rho_{bb}/\tau_{XX}$, $\langle i|\Gamma[\rho]|i\rangle = \rho_{bb}/2\tau_{XX} - \rho_{ii}/\tau_X$ ($i = x, y$), and $\dot{\rho}_{bb} + \dot{\rho}_{xx} + \dot{\rho}_{yy} + \dot{\rho}_{gg} = 0$. Except the off-diagonal damping rates, all parameters (ΔE_{xx} , $E_x - E_y$, d , τ_{XX} , τ_X) entering the equations are known experimentally. Therefore, though the set is relatively large, the population dynamics is fully defined and the Γ_{ij} , describing the coherence decay, can be deduced by comparing with the experimental data. The dynamical response is independent on whether $|x\rangle$ or $|y\rangle$ is addressed. Hence, $\Gamma_{xg} = \Gamma_{yg}$, $\Gamma_{bx} = \Gamma_{by}$, and making the reasonable assumption $\Gamma_{bx} = \Gamma_{xg} + \Gamma_{bg}$, the only two free parameters left are the exciton (Γ_{xg}) and biexciton (Γ_{bg}) decoherence rates.

We have numerically solved the equations for Gaussian pulse shapes assuming $\rho_{gg} = 1$ and all other $\rho_{ij} = 0$ before the TP pulse and taking the resultant ρ_{ij} as initial

values for the interaction with the ST pulse. In a time-integrated detection mode, the linear polarization degree is given by $\rho_L = (\delta\rho_{xx} - \delta\rho_{yy})/(\delta\rho_{bb} + \delta\rho_{xx} + \delta\rho_{yy})$, $\delta\rho_{ii}$ denoting the change of the population generated by the pulses. Calculating ρ_L as a function of the pulse delay yields indeed perfect agreement with experimental curves in Fig. 3c, verifying that the population dynamics is governed by the life-times τ_{XX} and τ_X . The decoherence rates follow from the density dependence of ρ_L (Fig. 3b). Too large rates spoil rapidly the purity of the TP excitation, resulting in a significant polarization degree even without the ST pulse, while the maximum level of only $\rho_L = 0.8$ signifies the presence of pure dephasing beyond the radiative damping. The fit to the data yields $\Gamma_{\text{bg}}^{-1} \approx \Gamma_{\text{bg}}^{-1} = 6$ ps. A careful analysis of the spectral line-shape of the exciton emission provides that the radiative Lorentzian is superimposed to a weak but broad acoustic phonon background, which translates in non-exponential damping in the time domain with a short component consistent with the rates deduced from the ST data (see also [15]). Distinct non-exponential damping is also indicated by TP coherent control measurements [8]. Here, a significant drop of the contrast occurs right after pulse separation, whereas the subsequent decay evolves on a much longer time-scale. Fig. 4 represents plots of the density matrix elements versus pulse area $\theta = \int_{-\infty}^{+\infty} \Omega(t)dt$ in the experimentally relevant pulse-density range. Despite of the relatively fast dephasing, the TP pulse creates a significant biexciton coherence ρ_{bg} that can be manipulated with the succeeding ST pulse. Damped Rabi oscillations have been already observed previously [2, 3, 16]. However, unlike our study, where we monitor an absolute quantity, no conclusions about the true coherence degree could be made.

Knowing the whole density matrix, the entanglement

of formation $E(\rho)$ can be calculated. Following Ref.[17], $E = E(C) = h(\frac{1+\sqrt{1-C^2}}{2})$ with the concurrence C and $h(x) = -x \log_2(x) - (1-x) \log_2(1-x)$. For a purely coherent regime, it is straightforward to show that $C = 2\sqrt{\rho_{\text{gg}}\rho_{\text{bb}}}$. While we can come with the TP pulse experimentally close to a situation $\rho_{\text{bb}} \approx \rho_{\text{gg}} \approx \frac{1}{2}$, the actual entanglement is markedly lower than 1. Decoherence establishes a mixed state, where now $C(\rho) = \max[0, \lambda_1 - \lambda_2 - \lambda_3 - \lambda_4]$, the λ 's being in decreasing order the square roots of $\rho\sigma_y \otimes \sigma_y \rho^* \sigma_y \otimes \sigma_y$ with the time inversion operator σ_y [17]. The calculation provides a maximum entanglement of about 0.5. However, this limited value given, complete disentanglement of the 2-quantum-bit system is accomplished by the ST pulse in a wide range of pulse areas (Fig. 4).

In conclusion, we have demonstrated entanglement and disentanglement of the electronic states of a QD by a sequence of two optical pulses. Being able to control the recombination path of the biexciton, the cascade emission can be adjusted from a pair of correlated or even entangled photons to a single photon of defined polarization or in an entangled polarization state. While an extrinsic background spoiling the figure-of-merit can be eliminated by appropriate sample design, our measurements uncover also rather large decoherence rates, probably related to a non-Markovian acoustic phonon contribution. This point deserves further investigations beyond the scope of this work. Our results are also of relevance for the use of QD in lasers, as they show that the exciton level is rapidly emptied avoiding reabsorption.

The authors thank S. Rogaschewski for the lithographic etching. This work was supported by the Deutsche Forschungsgemeinschaft within Project No. He 1939/18-1.

-
- [1] I. A. Nelson and I. L. Chang, *Quantum Computation and Quantum Information* (Cambridge University Press, UK, 2000).
 - [2] D. Gammon and D. G. Steel, *Phys. Today* **55**, 36 (2002) and references therein.
 - [3] X. Li et al., *Science* **301** 809 (2003).
 - [4] D. Gammon et al., *Phys. Rev. Lett.* **76**, 3005 (1996); M. Bayer et al., *Phys. Rev. Lett.* **82**, 1748 (1999).
 - [5] U. Hohenester, *Phys. Rev. B* **66**, 245323 (2003).
 - [6] E. Biolatti et al., *Phys. Rev. Lett.* **85**, 5647 (2000); P. Chen et al., *Phys. Rev. Lett.* **87**, 67401 (2001).
 - [7] Gang Chen et al., *Phys. Rev. Lett.* **88**, 117901 (2002).
 - [8] T. Fllissikowski et al., *Phys. Rev. Lett.* **92**, 227401 (2004)
 - [9] P. Michler et al., *Science* **290**, 2282 (2000); C. Santori et al., *Phys. Rev. Lett.* **86**, 1502 (2001).
 - [10] O. Benson et al., *Phys. Rev. Lett.* **84**, 2513 (2000).
 - [11] A. Barenco et al., *Phys. Rev. Lett.* **74**, 4083 (1995).
 - [12] D. Litvinov et al., *Appl. Phys. Lett.* **81**, 640 (2002).
 - [13] V. D. Kulakovskii et al., *Phys. Rev. Lett.* **82**, 1780 (1999); F. Kreller et. al, *Appl. Phys. Lett.* **74**, 2489 (1999).
 - [14] T. Fllissikowski et al., *Phys. Rev. Lett.* **86**, 3172 (2001).
 - [15] L. Besombes et al., *Phys. Rev. B* **63**, 155307 (2001); P. Borri et al., *Phys. Rev. Lett.* **87**, 157401 (2001); E. A. Muljarov and R. Zimmermann *Phys. Rev. Lett.* **93**, 237401 (2004).
 - [16] H. Kamada et al., *Phys. Rev. Lett.* **87**, 246401 (2001); P. Borri et al., *Phys. Rev. B* **66**, 81306(R) (2002); A. Zrenner et al., *Nature* **418**, 612 (2002); H. Htoon et al., *Phys. Rev. Lett.* **88**, 87401 (2002); L. Besombes et al., *Phys. Rev. Lett.* **90**, 257402 (2003); A. Muller et al., *Appl. Phys. Lett.* **84**, 981 (2004); J.M. Villas-Bôas et al., *Phys. Rev. Lett.* **94**, 57404 (2005); T. Unold et al., *Phys. Rev. Lett.* **94**, 137404 (2005).
 - [17] W. K. Wootters, *Phys. Rev. Lett.* **80**, 2245 (1998).